

Compliance in Gait Synthesis: Effects on Energy and Gait

Michael Scheint, Marion Sobotka, Martin Buss

Technische Universität München, Germany m.scheint@tum.de, marion.sobotka@tum.de, m.buss@ieee.org

Abstract—The role of compliance in walking controller synthesis is explored in this paper. Gait is designed for a simple biped with compliant legs using the concept of hybrid zero dynamics. Simultaneous optimization of gait and leg spring stiffness and optimization of gait at a fixed leg spring stiffnesses is carried out. Different cost functions based on energy are considered. The influence of compliance on gait and the influence of the measure of energy on optimal compliance are investigated.

It is shown that minimum actuator energy consumption is obtained if leg stiffness is subject to optimization along with gait parameters. Sum of actuator work and spring work is higher than in optimized stiff-legged gait. Depending on the choice of cost function, fundamental different gait characteristics and optimal stiffnesses are obtained.

I. INTRODUCTION

Today's most advanced robots such as the ASIMO [1] or HRP-2 [2] are very versatile robots achieving walking at 2.7 km/h or climbing stairs. Walking pattern and control is based on keeping the ZMP within the foot support area. The main drawback of this widely used approach is the poor walking energy efficiency achieved. The first version of ASIMO is reported to consume during walking more than 30 times the energy consumed by a human walking [3]. The challenge of energy efficiency can be addressed by several means. Promising approaches are passive dynamic walking and the use of springs.

The principle of passive dynamic walking was first investigated in [4]. Robots based on this principle include the Cornell biped, the most efficient mechanism for level-walking reported in literature [3]. A more sophisticated biped with 9 actuated joints, Flame [5], also uses the idea of passive dynamic walking. But most passive dynamic walkers are only capable of walking at a constant speed. Extending versatility for this class of robots is still an active field of research.

Studies analyzing human locomotion [6], [7] indicate another possibility to increase energy efficiency: the use of springs. Springs can be used to store and release energy, avoiding work done by the actuators. Several uses of springs in human walking have been reported in literature including support of leg swing at the hip [7] or pogo-stick like motion of the legs [7]. For the latter, studies on simple conservative models [6], [8] show how certain spring stiffnesses can lead to human like walking patterns.

Application of compliant elements such as springs for non-conservative biped walking has been studied in literature. Early examples include Waseda WL-13 [9], where a heuristically chosen spring was used to reduce energy consumption. More

recently, joint compliances for the pneumatic biped Lucy [10] were fitted to the derivative of reference torque to joint angle.

In [11] parallel hip springs were optimized simultaneously with polynomial reference trajectories. Necessary actuator power for a simple three link biped was reduced. Another optimization of gait and springs parallel to the joints was performed in [12] for an anthropomorphic 12 DOF biped. Flat-footed ZMP based walking was iteratively optimized for energy. Parallel springs in the knee were considered in [13], with gait optimized for three different spring stiffnesses.

Either spring properties were fixed or restricting assumptions on gait were made in most of the above mentioned publications. But how does stiffness as a degree of freedom in optimization influence gait if the latter is optimized for energy? This issue has not been addressed in detail to the authors' knowledge. Moreover, dependence of optimal gait and stiffness on the measure of energy needs to be investigated.

In order to address these questions, gait optimization is studied for a simple underactuated biped. Simplified models have been investigated previously [14] to reproduce certain characteristics of human walking. Here, the legs are compliant with springs in parallel to actuators. The method of hybrid zero dynamics [15], [16] is used to parametrize the optimal control problem. Advantages of this method include the applicability to underactuated bipeds, a simplified test for orbital stability and the possibility to optimize for energy consumption. Simultaneous optimization of gait and leg stiffness is performed with no a priori assumptions on step length, intermediate postures or similar.

The remainder of this paper is organized as follows. In chapter 1, the model of the considered biped is presented. Chapter 2 gives a brief summary on the method of hybrid zero dynamics. Cost functions are presented in chapter 3. In chapter 4, results of numerical optimization of gait are discussed. In chapter 5, conclusions are drawn from the presented results.

II. MODELING

A. General description

The biped model considered here is shown in Fig. 1. It consists of two legs and one torso with point masses located at the feet, center of the legs, hip and torso. The feet are assumed to be point feet, hence, the biped is underactuated in single support phases. The biped has four actuated joints, two at the hip and one at each leg. All actuators are considered to be massless and frictionless. At the legs, linear springs of

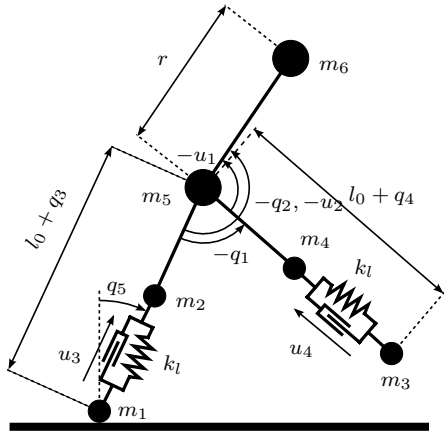


Fig. 1. Biped model with leg springs in parallel to leg actuators. Angles and torques are measured positive in clockwise direction.

stiffness k_l work in parallel to the actuators. As the foot mass is considered to be non-zero, this model is non-conservative for an inelastic ground model. The biped is an abstraction of a human body, motivated by the work in [6]. Similar stiff legged models have been used in [11], [17], [14].

Walking is modeled as a consecutive alternation of single support phases, also called stance phase, with one leg on the ground and instantaneous double support phases with both feet on the ground. Furthermore, walking is restricted to the saggital plane. Foot scuffing is not considered here, as the model has no knees.

The generalized coordinates \mathbf{q} of the stance phase constitute the state vector \mathbf{x} of the continuous system:

$$\mathbf{x} = \begin{bmatrix} \mathbf{q}^T & \dot{\mathbf{q}}^T \end{bmatrix}^T \quad \text{with} \quad \mathbf{q} = [q_1, q_2, q_3, q_4, q_5]^T. \quad (1)$$

With this choice of coordinates, the length of stance leg l_{stance} and swing leg l_{swing} are given as follows:

$$l_{\text{stance}} = l_0 + q_3 \quad \text{and} \quad l_{\text{swing}} = l_0 + q_4. \quad (2)$$

B. Dynamics of Single Support Phase

The equations of motion for the single support phase of the biped are derived using the Euler Lagrange approach [18]. By including springs, the potential energy does not consist of gravitational energy only but also includes energy stored in the springs.

$$V = \sum_{i=0}^6 m_i g p_{cm,i}^v + \frac{1}{2} k_l q_3^2 + \frac{1}{2} k_l q_4^2 \quad (3)$$

Here, $p_{cm,i}^v$ denotes the position of i -th point mass on the vertical axis and k_l denotes the leg spring stiffness. The equations of motion of the stance phase can be derived as:

$$\mathbf{D}(\mathbf{q}) \ddot{\mathbf{q}} + \mathbf{C}(\mathbf{q}, \dot{\mathbf{q}}) \dot{\mathbf{q}} + \mathbf{g}(\mathbf{q}) = \mathbf{B} \mathbf{u} - \mathbf{K} \mathbf{q} = \mathbf{B} \tilde{\mathbf{u}}(\mathbf{q}) \quad (4)$$

Here, \mathbf{D} denotes the inertia matrix, \mathbf{C} the matrix of Coriolis and centrifugal forces, \mathbf{g} the vector of gravitational forces, $\mathbf{K} = \text{diag}(0, 0, k_l, k_l, 0)$ the matrix of spring stiffnesses and

TABLE I
MODEL PARAMETERS

Foot mass	$m_1 = m_3$	1.0	kg
Leg mass	$m_2 = m_4$	4.0	kg
Hip mass	m_5	15.0	kg
Torso mass	m_6	10.0	kg
(Rest) Leg length	l_0	1.0	m
Torso length	r	0.5	m

\mathbf{B} a linear mapping of actuator input \mathbf{u} to the coordinates \mathbf{q} . For the special form of \mathbf{K} , a new input vector $\tilde{\mathbf{u}}$ can be defined, which is sum of force/torque input from the actuators \mathbf{u} and the springs $\mathbf{K} \mathbf{q}$.

Equation (4) can be transformed into standard state space notation of a nonlinear control affine system:

$$\dot{\mathbf{x}} = \mathbf{f}(\mathbf{x}) + \mathbf{G}(\mathbf{x}) \tilde{\mathbf{u}}. \quad (5)$$

C. Impact and Hybrid Model

For impact modeling, it is assumed that the collision of the swing leg with the ground is instantaneous and inelastic with no slip or rebound. Additionally, the former stance leg shall leave the ground just after impact.

Using the conservation of momentum while neglecting actuator inputs, an algebraic relation between the state right before \mathbf{x}^- and right after impact \mathbf{x}^+ can be derived. Combined with a relabeling operation on the state that exploits the symmetry of the biped, the impact equation is given as:

$$\mathbf{x}^+ = \Delta(\mathbf{x}^-). \quad (6)$$

It has to be noted, that the existence of parallel springs does not alter the impact map. With (6), a hybrid model for walking can be stated. The continuous dynamics of the single discrete state is given in (5). Impact with ground is the transition leading to a reset of the continuous state according to (6).

$$\Sigma = \begin{cases} \dot{\mathbf{x}} = \mathbf{f}(\mathbf{x}) + \mathbf{G}(\mathbf{x}) \tilde{\mathbf{u}} & \text{for } \mathbf{x}^- \notin \mathcal{S} \\ \mathbf{x}^+ = \Delta(\mathbf{x}^-) & \text{for } \mathbf{x}^- \in \mathcal{S} \end{cases} \quad (7)$$

The switching set \mathcal{S} is given by

$$\mathcal{S} = \{ \mathbf{x} \mid p_2^v(\mathbf{x}) = 0 \wedge p_2^h(\mathbf{x}) > 0 \}. \quad (8)$$

Swing foot position is denoted by p_2^v on the vertical and by p_2^h on the horizontal axis.

III. HYBRID ZERO DYNAMICS

The control method employed here is called ‘‘Hybrid Zero Dynamics’’ (HZD), which was developed in [15]. It provides a systematic approach for finding dynamically feasible and orbital asymptotical stable trajectories.

Only the main concepts of the hybrid zero dynamics from [16] are now summarized. Through a special choice of output functions and corresponding state feedback, system dynamics can be reduced to a two dimensional dynamics, the hybrid zero dynamics. Parameterization of the output function simplifies the optimal control problem, which is presented in the next section. Discussion is based on the hybrid model (7) of a biped with N degrees of freedom.

A. New Coordinates and Invariance

The concept of hybrid zero dynamics uses a special set of coordinates consisting of (relative) body angles \mathbf{q}_b and an absolute angle θ . The latter is the angle of the connection of the inertial frame to some point on the robot. Choice of θ is not fixed, but θ must be strictly increasing over one step when measured positive in clockwise direction. The transformation matrix \mathbf{H} maps original coordinates \mathbf{q} onto the new ones, with $\mathbf{H} = \mathbf{I}$ for coordinates chosen in Fig. 1.

$$\begin{bmatrix} \mathbf{q}_b \\ \theta \end{bmatrix} = \mathbf{H}\mathbf{q} \quad (9)$$

The actuated variables \mathbf{q}_b shall follow a desired trajectory given by $\mathbf{h}_d(\theta(t))$. Equivalently, an output function composed of \mathbf{q}_b and \mathbf{h}_d is required to be zero.

$$\mathbf{q}_b \stackrel{!}{=} \mathbf{h}_d(\theta) \Leftrightarrow \mathbf{y} = \mathbf{h}(\mathbf{q}) = \mathbf{q}_b - \mathbf{h}_d(\theta) \stackrel{!}{=} \mathbf{0} \quad (10)$$

Tracking the desired trajectory is now identical to zeroing the output functions. Zero outputs can be enforced through appropriate input/output linearizing state feedback:

$$\tilde{\mathbf{u}}(\mathbf{x}) = -(\mathcal{L}_f \mathcal{L}_g \mathbf{h}(\mathbf{q}))^{-1} \mathcal{L}_f^2 \mathbf{h}(\mathbf{q}). \quad (11)$$

If above state feedback is applied, the system state stays invariant with respect to the subset \mathcal{Z} of state space.

$$\mathcal{Z} = \{\mathbf{x} \mid \mathbf{h}(\mathbf{q}) = \mathbf{0} \wedge \mathcal{L}_f \mathbf{h}(\mathbf{q}) = \mathbf{0}\} \quad (12)$$

Control law (11) ensures invariance during stance phase. For obtaining the desired evolution \mathbf{h}_d for several steps, invariance must be achieved for the hybrid model. Thus, the output functions need to be impact invariant:

$$\Delta(\mathcal{S} \cap \mathcal{Z}) \subset \mathcal{Z}. \quad (13)$$

B. Zero Dynamics

Under feedback control (11) an internal dynamics in the unactuated angle θ and the angular momentum σ conjugate to θ exists. With (9) and $\mathbf{x} \in \mathcal{Z}$, the zero dynamics of the stance phase can be expressed as:

$$\begin{aligned} \dot{\theta} &= \kappa_1(\theta) \sigma \\ \dot{\sigma} &= \kappa_2(\theta). \end{aligned} \quad (14)$$

If the system (7) is kept in the set \mathcal{Z} by control (11), then equations (14) embed the dynamics of the complete system. Hence, the state \mathbf{x} can be calculated from $\theta, \dot{\theta}$ by (9)(10).

Assuming that the output functions \mathbf{h} comply with the requirement (13), the zero dynamics of the stance phase can be extended to a hybrid zero dynamics with state $\mathbf{z} = [\theta, \sigma]^T$. The transition taken at impact $\mathbf{z} \in (\mathcal{S} \cap \mathcal{Z})$ is:

$$\sigma^+(\mathbf{x}^-) = \delta_{\text{zero}}(\mathbf{x}^-) \sigma^-(\mathbf{x}^-). \quad (15)$$

Through further analysis, the scalar δ_{zero} can be identified to be the eigenvalue of the Poincaré map of (14).

If for the eigenvalue $0 < \delta_{\text{zero}}^2 < 1$ holds, then the periodic orbit of the hybrid zero dynamics is exponentially stable. Assuming a finite-time stabilizing controller for (10), then exponential stability of the reduced system (14) implies exponential stability of the full system (7).

C. Parameterization

In the design process of the hybrid zero dynamics method, the remaining degree of freedom is the choice of \mathbf{h}_d . The choice made here are Bézier polynomials, which simplify calculations e.g. in ensuring (13). Desired evolution $h_{d,i}$ of angle $q_{b,i}$ is now a Bézier polynomial in θ of degree M .

$$h_{d,i} = \sum_{k=0}^M \alpha_k^i \frac{M!}{k!(M-k)!} s^k (1-s)^{M-k} \quad (16)$$

$$\text{with } s = s(\theta) = \frac{\theta - \theta^-}{\theta^+ - \theta^-} \quad (17)$$

The trajectories of $\mathbf{q}_b \in \mathbb{R}^{N-1}$ and the hybrid zero dynamics are now parameterized by the $(N-1)(M+1)$ coefficients α_k^i of the Bézier polynomials. Ensuring impact invariance (13) reduces the number of independent parameters for each polynomial by two. The remaining parameters are combined in the parameter vector $\boldsymbol{\alpha} \in \mathbb{R}^{(N-1)(M-1)}$.

$$\boldsymbol{\alpha} = [\alpha_2^1, \dots, \alpha_M^1, \dots, \alpha_2^{N-1}, \dots, \alpha_M^{N-1}] \quad (18)$$

IV. OPTIMIZATION PROBLEM

Using the parameterization in (16) and the overall concept of the hybrid zero dynamics, the general optimal control problem is reduced to a nonlinear programming problem (NLP). In the first part of this section, the general optimization problem is presented, with the discussion of possible cost functions left to the second part.

A. General

As given in (12),(11), the evolution of the state $\mathbf{x}(t)$ and input $\tilde{\mathbf{u}}(t)$ is given by $\theta(t), \sigma(t)$ on the hybrid zero dynamics. Hence, evaluation of the full system dynamics is reduced to the evaluation of the hybrid zero dynamics parameterized by $\boldsymbol{\alpha}$. The general optimization objective is then given in terms of $\boldsymbol{\alpha}, k_l$ with a set of nonlinear inequality constraints.

$$\min_{\boldsymbol{\alpha}, k_l} J(\boldsymbol{\alpha}, k_l) \quad (19)$$

Optimization shall yield a orbital stable gait, hence, the inequality $0 < \delta_{\text{zero}}^2 < 1$ is required to hold. Average speed over one step, i.e. the ratio of step length L_s and step time t_s , should be greater than or equal to the desired speed v_{des} . Speed v_{des} may not be exceeded by more than δv_{des} . Hence, speed is confined to: $v_{des} \leq \frac{L_s}{t_s} \leq v_{des} + \delta v_{des}$.

Moreover, force from the ground at the stance foot must be unilateral ($F_1^v > 0$). Throughout one step, stance foot forces must be within the friction cone $|F_1^h/F_1^v| < \mu$. Impact modeling requires the former stance foot with position p_2 to lift off the ground $\dot{p}_2^y(t^+) > 0$ after impact at $t = t_c$. The forces F_2^v, F_2^h at the swing leg at impact have to be in the friction cone $|F_2^h(t_c)/F_2^v(t_c)| < \mu$ and unilateral $F_2^v > 0$. Further constraints not explicitly stated here ensure the existence of the hybrid zero dynamics.

Optimization was performed under Matlab using the SQP-based *fmincon* solver of the optimization toolbox. The following parameter values were used in optimization: $v_{des} = 0.8 \frac{\text{m}}{\text{s}}$, $\delta v_{des} = 0.05 \frac{\text{m}}{\text{s}}$, $\mu = 0.6$ and $M = 4$.

TABLE II
OPTIMIZATION RESULTS FOR $k_l = 0$ AND $k_l = k_{l,opt}$

Cost function	$k_l = 0$	$k_l = k_{l,opt}$	$J(k_{l,opt})/J(k_l = 0)$
J_1	299.27	7.5870	0.0254
J_2	0.0726	0.0578	0.7965
J_3	1.2976	0.1437	0.1107

B. Cost Functions

Three different cost functions are considered in this investigation and are presented in this subsection. All cost functions are normalized with respect to weight and distance travelled.

If all actuators are considered to be electric motors, one possible measure of energy is the energy loss in the coils of the motor. Current is approximately proportional to torque/force, hence, the integral of the squared torques/forces is a measure of these heat losses yielding cost function J_1 .

$$J_1 = \frac{1}{mgL_s} \int_{t=0}^{t_s} \|\tilde{\mathbf{u}}(\theta(t), \sigma(t), k_l)\|_2^2 dt \quad (20)$$

The second cost function is the specific mechanical cost of transport (c_{mt}). Note that only the absolute values of the mechanical power are integrated. The underlying assumption is that electric motors are usually not able to recover energy from negative work (braking).

$$J_2 = \frac{1}{mgL_s} \int_{t=0}^{t_s} \|\dot{\mathbf{q}}(\theta(t), \sigma(t))^T \mathbf{B} \tilde{\mathbf{u}}(\theta(t), \sigma(t), k_l)\|_1 dt \quad (21)$$

Finally, a third cost function is proposed which is the weighted sum of J_1 and J_2 . It is used to investigate the existence of a gait which minimizes both J_1 and J_2 or which has unique characteristics. Moreover, this cost function is possibly closer to the actual energy consumption of an electric motor.

$$J_3 = \gamma J_1 + J_2 \quad \text{with} \quad \gamma = 0.0032. \quad (22)$$

For this paper, the weighting constant γ is chosen such that neither J_1 nor J_2 dominate the cost functional. The influence of γ on the resulting gait characteristics is discussed in the next section.

V. RESULTS

In this section results from numerical optimization of (19) are presented. First, results of simultaneous optimization of gait parameters α and leg spring stiffness k_l are compared to the case of optimization of α with $k_l = 0$. Next, optimization approaches are discussed which impose additional constraints to the original problem. Optimized gait is analyzed with respect to center of mass (CoM) trajectory and ground reaction force (GRF). Finally, actuator inputs and spring forces are compared for the stance leg.

One necessary premise for the discussion on optimal costs is that the results are comparable, i.e. they represent a minimum

in costs that is close to a potential global one. As the SQP based solver only delivers local minima, a set of initial gait parameters α and a set of initial spring stiffnesses k_l are used for each optimization case. The best result is selected in each case and considered as ‘‘global’’ optimum for the discussion.

A. Zero and Optimal Stiffness

Optimization was carried out for each cost function (20)-(22) for two cases. First, leg stiffness was set to zero ($k_l = 0$) and only gait was optimized. In the other case, stiffness k_l was an additional parameter in optimization, as indicated in (19). Best results are summarized in Table II.

The largest reduction in costs appears for cost function J_1 . Walking optimized for J_1 with zero stiffness is approx. 40 times more expensive than walking with optimized leg stiffness. For cost function J_2 , the optimized springs reduce costs only by 20%. One possible reason lies in the fact that J_2 can be minimized by reducing either required force u_i or joint velocity \dot{q}_i . For the second strategy, a spring cannot help to reduce costs further.

When optimizing both α and k_l for J_1 , the costs measured by J_2 are also reduced by 94% to 0.1364. But this absolute value for J_2 is twice the value obtained when optimizing for J_2 . Similar results are found when examining optimization with respect to J_2 . Cost function J_1 gets reduced by 91%, the resulting absolute value being 37.17.

In order to improve both costs J_1 and J_2 , the third cost function J_3 , a weighted sum of J_1 and J_2 is now considered. A range of weighting factors γ is examined. For γ being above 0.004, the contribution J_1 dominates J_3 , yielding an optimization result similar to the one obtained when optimizing for J_1 . A similar domination of J_2 occurs for γ smaller than 0.003. Only for a small range of γ , e.g. $\gamma = 0.0032$, both components of J_3 are approximately equally contributing to the costs. This results in gait characteristics and an optimal stiffness $k_{l,opt}$ in between the two extremes.

Costs obtained from optimizing both gait and stiffness for J_3 are given in Table II. Thereby, J_2 contributes 63% to total costs, γJ_1 contributes 37%. The absolute value of J_1 is 16.81, the one of J_2 0.0899. Hence, the goal of reducing costs with respect to both J_1 and J_2 is achieved even if the absolute values are still above the best possible values. But this result is very sensitive to the choice of γ . Furthermore, as the resulting gait from J_3 does not show unique characteristics but averages features of J_1 and J_2 , for the remainder of this paper only the cost functions J_1 and J_2 are discussed.

B. Optimization with Additional Restrictions

In this subsection, three cases are considered where the optimization problem in (19) is additionally restricted or modified. The first case is to perform optimization with k_l fixed. The results for a range of k_l values are shown in Fig. 2. The evolution of optimal costs with respect to k_l verify the results from Table II, which are marked by triangles. Stiffness values $k_{l,opt}$ obtained from simultaneous optimization of gait and stiffness agree with potential least cost regions which can

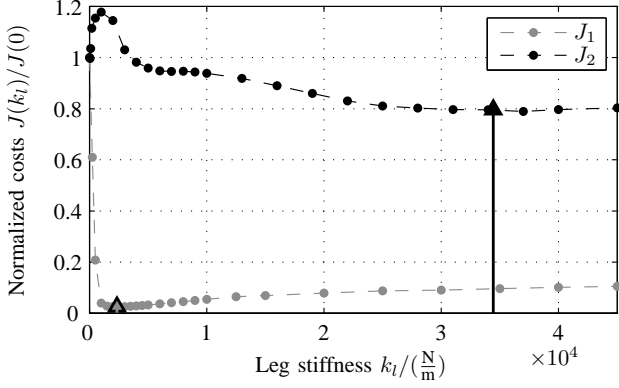


Fig. 2. Optimal cost values for each cost function for optimization where k_l is fixed to respective value. Costs are shown normalized with respect to costs at $k_l = 0$. Triangle markers show values for simultaneous optimization of k_l and α as given in Table II.

be identified in Fig. 2. Optimization over a grid of fixed leg stiffnesses can also find gait and stiffness pairs with costs close to a global minimum, but compared to simultaneous optimization of gait and stiffness a larger amount of computation is needed.

In the second case, optimization in (19) is split up in two subsequent ones. First, gait is optimized with leg stiffness set to zero. Then, only spring stiffness k_l is optimized for the given gait. For cost function J_1 , resulting spring stiffness is $k_l = 0$ as the fixed gait does not facilitate the spring usage. A spring stiffness of $k_l = 31.1 \frac{\text{N}}{\text{m}}$ is found to be optimal for cost function J_2 here, resulting in a very small reduction of 0.4% in costs. It can be observed from these results, that subsequent optimization of stiffness is not meaningful here.

In the last case, a specified pose at double support is required. This can be formulated as an additional constraint on (19). The pose was chosen to be $\mathbf{q} = [-\frac{\pi}{6}, -\pi, 0, 0, \frac{\pi}{12}]$. Optimization of gait parameters α and leg stiffness k_l results in costs of 13.81 in case of J_1 and costs of 0.087 in case of J_2 . The additional imposed constraint leads to an increase in costs of 50% to 80% compared to the results shown in Table II. This example shows that narrowing the search space of optimization by additional restrictions increases energy consumption, eventually even offsetting savings from using springs as in the case of J_2 .

C. CoM Trajectory and GRF

The vertical motion of the center of mass (CoM) for one step is shown in Fig. 3 for optimized stiffness $k_l = k_{l,opt}$ (top left) and zero stiffness $k_l = 0$ (top right). In case of zero spring stiffness, the trajectory for all cost functions is similar to the one of an inverted pendulum. For optimized stiffness, the gait optimized for J_2 shows a similar CoM vertical motion. Thus, not only does the compliance have relatively little effect on costs when optimizing for J_2 , but gait remains similar as well.

In contrast, the vertical CoM motion for J_1 changes drastically after optimization of stiffness. Motion resembles the one of a spring mass system. This can also be seen from the

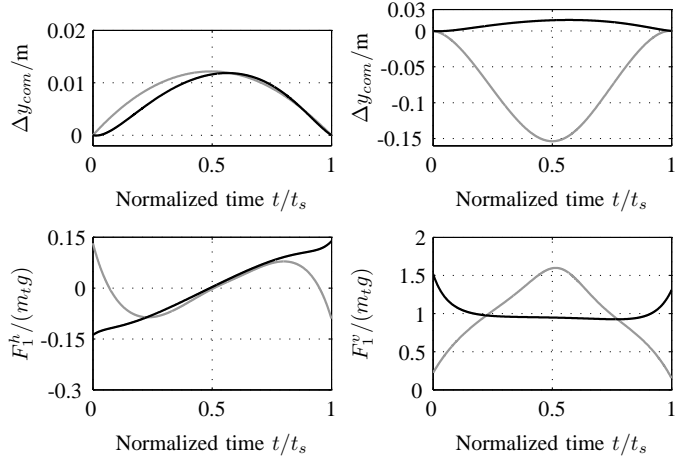


Fig. 3. Top row: Vertical displacement of CoM from impact height for $k_l = 0$ (left) and $k_l = k_{l,opt}$ (right). Cost function J_1 in gray, J_2 in black. Bottom row: GRF normalized by total weight over time for optimized stiffness. Left horizontal component F_1^h , right vertical component F_1^v . Colors as above. Time t is normalized with step time t_s .

vertical ground reaction force, given in the bottom right plot of Fig. 3. Another interesting measure for comparison is the maximum amount of potential energy stored in the stance leg spring. In case of optimization w.r.t. J_1 , the maximum energy is 60.7J, whereas in case of J_2 the maximum is only 3.4J. Hence, the optimized gait and stiffness for cost function J_1 results in a significant energy storage and release in the stance leg spring.

D. Actuation in the Stance Leg

The impact of the optimized leg springs on actuation in the leg and, consequently, on energy consumption is now discussed. Discussion focuses on actuation in the stance leg as actuation there is the major contributor to costs. In Fig. 4 actuation \tilde{u}_3 is shown for both zero and optimized stiffness. In the top plot, the resulting force inputs are shown for optimization with cost function J_1 . Necessary input from the motor u_3 is substantially reduced from stiffness $k_l = 0$ to optimized leg spring $k_{l,opt}$. The major part of leg actuation is then delivered by the spring with $k_l = k_{l,opt}$.

But total actuation for optimized stiffness is significantly higher than for zero stiffness. This is supported by evaluating the cost function J_1 for total actuation \tilde{u}_3 , i.e. neglecting work done by the spring. For the gait with optimized stiffness $k_{l,opt}$, this yields a value of 448.2. This value is about 1.5 times higher than the one obtained from optimizing with zero stiffness shown in Table II.

Hence, optimizing gait and leg stiffness for J_1 results in a higher energy throughput compared to optimization with zero stiffness. It can be concluded for cost function J_1 , that gait and compliance cannot be optimized independently from each other for lowest motor actuation cost. Gaits optimized simultaneously with stiffness k_l are clearly non-optimal with respect to evaluation of costs with zero stiffness.

For the cost function J_2 , actuation in the stance leg is shown

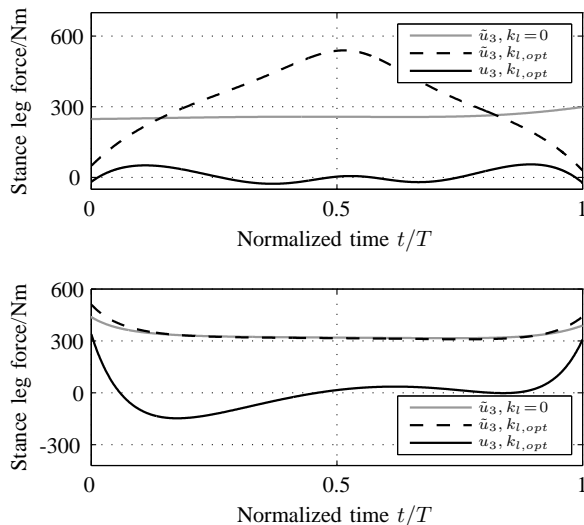


Fig. 4. Stance leg actuation for optimization with J_1 (top) and J_2 (bottom). Motor input u_3 in gray for $k_l = 0$ and in black for $k_{l,opt}$. Total input for $k_{l,opt}$ depicted by black dashed line.

in the lower plot of Fig. 4. Total actuation \tilde{u}_3 for optimized leg stiffness is nearly identical to \tilde{u}_3 for zero stiffness. Motor actuation u_3 is reduced when optimizing stiffness k_l . But in the first third of the stance phase, the motor significantly acts against the spring. This shows once again, that for cost function J_2 potential energy storage of the spring is not fully exploited.

VI. CONCLUSIONS

The influence of compliance in gait synthesis is analyzed in this paper for a simple biped. Effects on gait and energy depend on the choice of cost function.

For a cost function based on heat loss in a motor, the addition of leg stiffness to the optimization parameters leads to a fundamental different gait. A spring-mass model like gait is obtained, where the leg spring is exploited for energy storage and return. Costs of locomotion are drastically reduced, as the spring is responsible for most of the actuation in the leg.

Optimization of gait and stiffness for a mechanical work-based cost function does not alter gait significantly compared to optimization of gait only. The spring is not fully exploited, optimal spring stiffness is very high. Only rather small reductions in costs can be observed. For a rotational joint with parallel compliance, significant energy reductions are reported in [13] when optimizing gait for mechanical work. Therefore, a study on a biped with rotary joints could clarify whether the findings of this paper can be generalized.

The results in this paper can be used as principal guidelines for gait synthesis on a real biped with compliance. Simultaneous optimization of stiffness and gait is clearly advantageous. Costs should be based on motor heat loss. Artificial restrictions such as an initial pose can result in higher energy consumption.

Further investigations will concentrate on the influence of

a double support phase on gait and stiffness. In [14] a human like ground reaction force pattern was observed for similar model with double support.

ACKNOWLEDGMENT

This work is supported in part within the Grant WO1440/2-1 of the German Research Foundation (DFG). The authors thank Thomas Schauß for his help on the implementation of the hybrid zero dynamics optimization.

REFERENCES

- [1] Honda Motor Co., Ltd. (2008), "ASIMO." [Online]. Available: <http://world.honda.com/ASIMO/>
- [2] K. Kaneko, F. Kanehiro, S. Kajita, H. Hirukawa, T. Kawasaki, M. Hirata, K. Akachi, and T. Isozumi, "Humanoid robot HRP-2," in *Proceedings of the IEEE International Conference on Robotics and Automation (ICRA)*, vol. 2, 2004, pp. 1083–1090.
- [3] S. Collins, A. Ruina, R. Tedrake, and M. Wisse, "Efficient Bipedal Robots Based on Passive-Dynamic Walkers," *Science*, vol. 307, no. 5712, pp. 1082–1085, 2005.
- [4] T. McGeer, "Passive Dynamic Walking," *The International Journal of Robotics Research*, vol. 9, no. 2, pp. 62–82, 1990.
- [5] D. Hobbelen, "Limit cycle walking," Ph.D. dissertation, Technische Universiteit Delft, Delft, Netherlands, 2008.
- [6] H. Geyer, A. Seyfarth, and R. Blickhan, "Compliant leg behaviour explains basic dynamics of walking and running," *Proc R. Soc. B*, vol. 273, no. 1603, pp. 2861–2867, Nov 2006.
- [7] R. M. Alexander, "Three uses for springs in legged locomotion," *The International Journal of Robotics Research*, vol. 9, no. 2, pp. 53–61, 1990.
- [8] D. Owaki, K. Osuka, and A. Ishiguro, "On the embodiment that enables passive dynamic bipedal running," in *Proc. IEEE International Conference on Robotics and Automation (ICRA)*, Pasadena, CA, USA, May 2008, pp. 341–346.
- [9] J. Yamaguchi, D. Nishino, and A. Takanishi, "Realization of dynamic biped walking varying joint stiffness using antagonistic driven joints," in *Proceedings of the IEEE International Conference on Robotics and Automation (ICRA)*, vol. 3, 16–20 May 1998, pp. 2022–2029.
- [10] B. Vanderborght, B. Verrelst, R. Van Ham, M. Van Damme, D. Lefeber, B. M. Y. Duran, and P. Beyl, "Exploiting Natural Dynamics to Reduce Energy Consumption by Controlling the Compliance of Soft Actuators," *The International Journal of Robotics Research*, vol. 25, no. 4, pp. 343–358, 2006.
- [11] V. Duindam and S. Stramigioli, "Optimization of mass and stiffness distribution for efficient bipedal walking," in *Proceedings of the International Symposium on Nonlinear Theory and its Applications*, Bruges, Belgium, 2005.
- [12] T.-Y. Wu and T.-J. Yeh, "Optimal design and implementation of an energy-efficient, semi-active biped," in *Proceedings of the IEEE International Conference on Robotics and Automation (ICRA)*, Pasadena, CA, USA, May 2008, pp. 1252–1257.
- [13] T. Yang, E. Westervelt, and J. Schmiedeler, "Using parallel joint compliance to reduce the cost of walking in a planar biped robot," in *Proceedings of the 2007 ASME International Mechanical Engineering Congress and Exposition*, Seattle, Nov. 2007.
- [14] S. Miyakoshi, G. Cheng, and Y. Kuniyoshi, "Transferring human biped walking function to a machine - towards the realization of a biped bike," in *clawar*, September 2001, pp. 763–770.
- [15] E. Westervelt, J. Grizzle, and D. Koditschek, "Hybrid zero dynamics of planar biped walkers," *IEEE Trans. Automat. Contr.*, vol. 48, no. 1, pp. 42–56, 2003.
- [16] E. Westervelt, J. Grizzle, C. Chevallerau, J. Choi, and B. Morris, *Feedback control of dynamic bipedal robot locomotion*. Boca Raton: CRC Press, 2007.
- [17] J. Grizzle, G. Abba, and F. Plestan, "Asymptotically stable walking for biped robots: analysis via systems with impulse effects," *IEEE Trans. Automat. Contr.*, vol. 46, no. 1, pp. 51–64, 2001.
- [18] M. Spong, S. Hutchinson, and M. Vidyasagar, *Robot Modeling and Control*. Hoboken, NJ: Wiley & Sons, 2005.